https://doi.org/10.33271/nvngu/2026-5/163

Lam Thang Dinh[1],
orcid.org/0009-0005-0077-7965,
Thi Thu Hien Dinh[*2],
orcid.org/0009-0000-3720-9623,
Xuan Truong Tran[3],
orcid.org/0000-0003-4051-0307,
Van Binh Do[3],
orcid.org/0009-0009-8243-1288

1 – Institute for Mechanical, Automation and Environmental Science and Technologies, Hanoi, Vietnam
2 – Electric Power University, Hanoi, Vietnam
3 – Hanoi University of Mining and Geology, Hanoi, Vietnam
* Corresponding author e-mail: hiendtt@epu.edu.vn

APPLICATION OF GOOGLE EARTH ENGINE TO AUTOMATED SURFACE WATER QUALITY MONITORING IN THE RED RIVER AND DUONG RIVER BASINS

Purpose. To develop an automated cloud-based application to monitor surface water quality using Google Earth Engine and multi-source satellite imagery for major river systems, with application to the Red River and Duong River in Vietnam.

Methodology. The study was conducted using multi-source satellite data from Sentinel-2 MSI and Landsat 8/9 within the Google Earth Engine environment. Sentinel-2 MSI imagery was used to estimate total suspended solids (TSS) and water turbidity, whereas the thermal bands of Landsat 8/9 were used to calculate water surface temperature. Data processing included filtering satellite imagery by study area and acquisition period, spectral analysis, calculation of the relevant water quality parameters, and cartographic visualization of their spatial distribution. The satellite-derived values were compared with field measurements collected along the Red River and Duong River sections within Hanoi, Vietnam.

Findings. The results showed distinct spatial and seasonal patterns of TSS, turbidity, and water surface temperature. Comparisons with field measurements demonstrated acceptable agreement between satellite-derived estimates and observed data, supporting the applicability of the proposed approach for river-basin-scale water quality assessment.

Originality. This study presents an integrated Google Earth Engine-based framework that combines multi-source remote sensing data with field observations to support automated, scalable surface water quality monitoring in Vietnam.

Practical value. The developed application can be applied efficiently for rapid, scalable, and cost-effective water quality monitoring, particularly in data-scarce regions and large river basins where conventional monitoring networks are insufficient.

Keywords: *Google Earth Engine, remote sensing, water quality, total suspended solids, turbidity, river basin*

Received: 28 May 2026
Accepted: 17 August 2026
Available online: 27 October 2026

Introduction. Surface water is a critical natural resource, playing an essential role in socioeconomic development, environmental security, and human quality of life [1]. Amid population growth, rapid urbanization, and industrial development, surface water quality in many river basins is deteriorating, particularly in urban and downstream areas [2]. Industrial and mining activities can further alter the hydrochemical characteristics of surface waters, particularly in areas affected by mineral extraction and mine drainage [3]. Therefore, regular, continuous monitoring and assessment of surface water quality are urgent requirements for water resource management and environmental protection. Monitoring surface water quality provides an important scientific basis for evaluating the current state of the aquatic environment, identifying spatial and temporal trends in transformation, and supporting pollution warning, prevention, and control efforts [4, 5]. Recent studies of river systems have also demonstrated the importance of suspended-matter monitoring for identifying temporal changes in surface-water conditions [6]. Information on water quality helps managers make timely decisions on water resource planning, waste source control, and the protection of aquatic ecosystems [7]. For river systems with complex hydrological regimes and strong seasonal

© Lam Thang Dinh, Thi Thu Hien Dinh, Xuan Truong Tran, Van Binh Do, 2026

fluctuations, water quality monitoring must be conducted at high frequency and across a broad spatial scale [8].

In practice, surface water quality monitoring is commonly conducted using traditional observation methods, including on-site water sampling and laboratory analysis [9, 10]. Although this approach yields high-precision results, it is time-consuming, costly, labor-intensive, and difficult to scale across large spatial areas [11]. In addition, modeling and statistical analysis methods have been used to assess and predict water quality [12, 13]. The integration of monitoring data with GIS technology is also used to assess surface water quality [14]. While this approach is simple and enables rapid implementation, accurate interpolation of water-quality parameter concentrations requires a sufficiently large and evenly distributed set of sampling points across the river basin or lake. However, the effectiveness of these methods depends heavily on the quantity and quality of input data [15]. In recent years, remote sensing has become an effective tool for surface water quality monitoring due to its ability to acquire simultaneous information over large areas and long time series. Combining remote sensing data with field monitoring data improves monitoring efficiency and reduces costs compared to traditional methods [16, 17].

Google Earth Engine (GEE) is a cloud computing platform that enables the storage, processing, and analysis of vast amounts of multi-source remote sensing data [18]. A prominent advantage of GEE is its ability to rapidly access global satellite datasets, perform online image processing, and develop real-time monitoring applications. Using GEE significantly reduces data processing time, eliminates the need for high-end hardware infrastructure, and enables the automation of analytical workflows [19]. Globally, numerous studies have applied the GEE platform to water quality monitoring. A recent study reviewed AI-based GEE applications for surface water monitoring, assessment, and management, suggesting that GEE provides fast and accurate insights for these purposes [20]. Furthermore, [21] conducted a systematic review of quantitative and qualitative water resources assessment methods using GEE, providing a comprehensive synthesis of current methodologies, data sources, and analytical frameworks. While [22] used GEE and spectral indices to monitor ex situ water quality in Chilika Lake, Odisha, India, [23] used a satellite-based GEE approach to assess water quality at the Mukutmanipur Dam. In addition, to analyze the spatio-temporal trends of water quality parameters in the Anzali lagoon, a multi-sensor framework in GEE was applied in [24]. Adopting a similar methodology, [25] concluded that GEE is an efficient, stable, and highly scalable platform for long-term monitoring of hydrological dynamics and water quality. GEE is particularly valuable in data-scarce regions, as it facilitates the generation of surface water and water quality products with high spatio-temporal resolution, supporting sustainable water resource management and environmental monitoring.

In Vietnam, the use of the GEE platform for water quality monitoring remains limited and has not been widely implemented. Existing studies primarily focus on individual parameters or have yet to develop intuitive applications for management purposes. Most of these efforts are dedicated to monitoring reservoir operations within river basins [26] or tracking fluctuations in riverbanks [27]. Despite numerous domestic and international studies on the application of remote sensing and GEE for water quality monitoring, several research gaps remain. Specifically, there is a lack of studies that fully integrate multi-temporal remote sensing data, field monitoring data, and cloud computing platforms to develop automated and intuitive water quality monitoring applications. In particular, for major river basins in Vietnam, the development of GEE-based water quality monitoring applications has not yet been systematically researched. Addressing these issues, this study aims to develop a water quality monitoring application on the Google Earth Engine platform that integrates remote sensing imagery and field observation data. The application is validated through a case study in the Red River and Duong River basins, contributing to the assessment of GEE's applicability to surface water quality monitoring at the river-basin scale.

Study area. The study area encompasses segments of the Red River and the Duong River that flow through Hanoi and its surrounding regions (Fig. 1). This area is characterized by high population density and numerous industrial zones, craft villages, and urban areas, and consequently faces significant pressure from domestic and industrial waste.

Wastewater from socio-economic activities and production processes in traditional craft villages is predominantly discharged directly into the environment, including the Red River and Duong River systems. These discharges have been the primary drivers of increasingly complex surface water pollution in these rivers in recent years. The Red River segment passing through Hanoi is approximately 120 km [28, 29]. The Red River's annual discharge is about 112 m^3, corresponding to an average annual flow rate of 3,560 m^3/s, with contributions from the Da River (48 %), Lo River (30 %), and Thao River (22 %). Upon reaching Hanoi, the Red River bifurcates into the Duong River, diverting approximately 28–30 % of its flow to the Thai Binh River system. The Red River's hydrological regime is divided into two distinct seasons: the flood season from May to October and the dry season from November to the following April. The Duong River is a distributary of the Red River, spanning 65 km and connecting two major river systems: the Red River and the Thai Binh River. It branches off from the Red River at Ngoc Thuy Ward (Gia Lam District), then flows east and southeast through Thuan Thanh and Gia Luong districts (Bac Ninh province), before joining the Thai Binh River at Dai Than, near Pha Lai. The segment of the Duong River flowing through Hanoi is 17.5 km long.

Data and methodology. *Remote sensing data*. The study uses two Landsat 8/9 images: a Landsat 8 image captured on September 6, 2024 (rainy season) and a Landsat 9 image captured on December 19, 2024 (dry season). The Thermal Infrared channel (Band 10) is used to calculate the water surface temperature for December 19, 2024, Landsat 8 image. (Fig. 2).

Monitoring data and spectral measurements. To assess surface water quality, 56 water samples were collected from segments of the Red River and the Duong River that flow through Hanoi. Of these, 43 points were used to develop regression functions, and 13 were reserved to

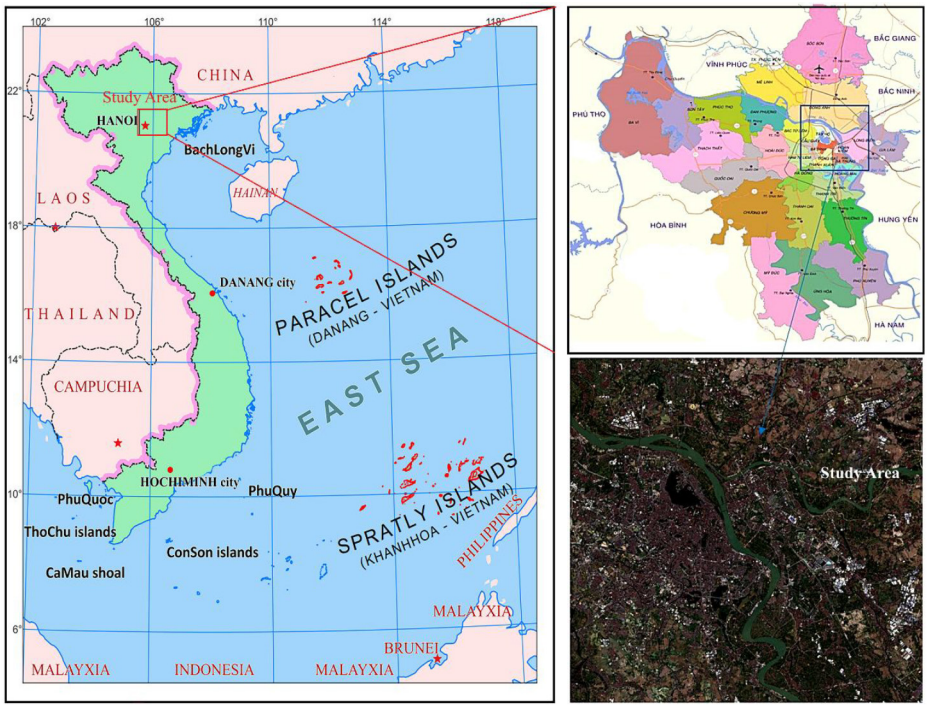

Fig. 1. Location of the study area in the Red River and Duong River basins, Vietnam

validate the accuracy of the established models. The spatial distribution of the sampling points within the study area is shown in Fig. 3.

Surface water samples were collected at the same locations as the field spectral reflectance measurements. Samples were taken from the surface layer at depths of 0–25 cm, because water below 25 cm does not affect surface reflectance [30]. Sampling points were evenly distributed across the study area to ensure a representative distribution of water-quality parameter concentrations. Water samples were stored in dark plastic bottles, kept chilled, and transported to the laboratory for analysis the same day. Sampling, preservation, and analysis were conducted in accordance with the National Technical Regulation on Surface Water Quality (QCVN 08-MT:2015/BTNMT). Analytical data for water-quality parameters were divided into two groups: one for building regression models and the other for evaluating the accuracy of the regression results.

The study selected five water quality parameters for analysis, including turbidity, total suspended solids (TSS), Chemical Oxygen Demand (COD), Biochemical Oxygen Demand (BOD5), and Ammonium (NH4+). In addition, a GER 1500 field spectroradiometer was used to measure the spectral reflectance of the water surface at the sampling locations. The GER 1500 measures the electromagnetic spectrum at the water surface from ultraviolet (UV) to near-infrared (NIR), specifically from 350 to 1,050 nm. It features up to 512 spectral channels with a spectral resolution of 1.5 nm. To ensure accuracy, the coordinates of the water quality sampling points were determined using a high-precision GPS device. Water surface reflectance measurements were conducted simultaneously with water sampling on December 11, 2023.

Developing a water quality monitoring application on the Google Earth Engine platform. GEE is a cloud computing platform for remote sensing data analysis that in-

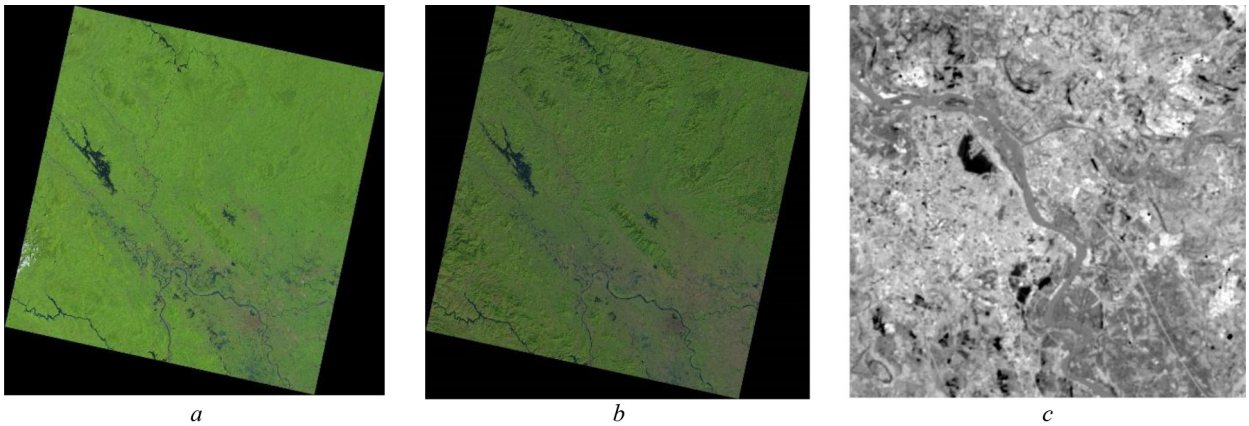

a *b* *c*

Fig. 2. Landsat imagery of the study area:

a – Landsat 8 OLI/TIRS image acquired on September 6, 2024; b – Landsat 9 OLI/TIRS image acquired on December 19, 2024; c – Landsat 9 thermal infrared Band 10 image acquired on December 19, 2024

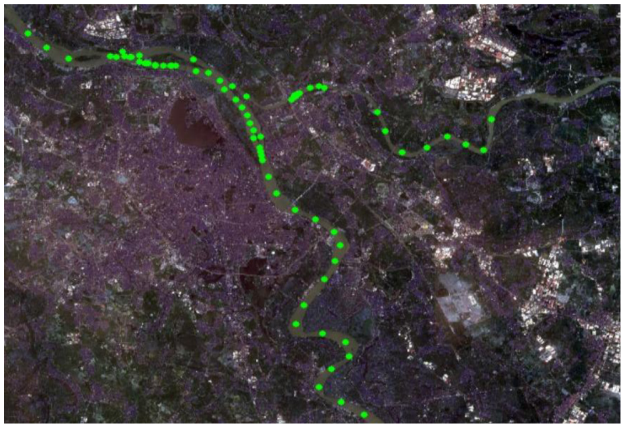

Fig. 3. Locations of surface-water sampling sites along the Red River and Duong River

tegrates a repository of tens of petabytes of free remote sensing data, including Landsat and Sentinel imagery. Typically, downloading and processing multi-temporal remote sensing images over a large study area is time-consuming and requires high-performance computing systems and expensive commercial image-processing software. However, with the GEE platform, these computations are significantly faster because data processing runs in parallel on Google's server infrastructure [18].

This study uses the JavaScript programming language in the Code Editor interface to import imagery into the platform and to perform processing, analysis, visualization, and export of results. Landsat 8/9 and Sentinel-2 MSI image collections are used to extract information on surface water quality parameters. The image data is then filtered by region and study period to reduce processing time. The program code for extracting water quality parameters from remote sensing data on the GEE platform is shown in Fig. 4. The tool interface is illustrated in Fig. 5.

```
var green_band_label = ui.Label('Green', LABEL_STYLE);
var U_green_band = ui.Select({items: bands, style: SELECT_STYLE, placeholder: 'B2', value: 'B2'}-+);
greenPanel.add(green_band_label).add(U_green_band);

var bluePanel = ui.Panel({style: {backgroundColor: colors.transparent}});
var blue_band_label = ui.Label('blue', LABEL_STYLE);
var U_blue_band = ui.Select({items: bands, style: SELECT_STYLE, placeholder: 'B3', value: 'B3'});
bluePanel.add(blue_band_label).add(U_blue_band);

var grayPanel = ui.Panel({style: {backgroundColor: colors.transparent}});
var gray_band_label = ui.Label('Grey - (1 kênh)', LABEL_STYLE);
var U_gray_band = ui.Select({items: bands, style: SELECT_STYLE, placeholder: 'B1', value: 'B1'});
grayPanel.add(gray_band_label).add(U_gray_band);

var RGBPanel = ui.Panel({layout: ui.Panel.Layout.flow('horizontal'), style: {backgroundColor: colors.transparent}});
var GrayPanel = ui.Panel({layout: ui.Panel.Layout.flow('horizontal'), style: {backgroundColor: colors.transparent}});
```

Fig. 4. Google Earth Engine JavaScript code for estimating surface-water quality parameters from satellite imagery

The software tool allows users to select various remote sensing datasets, including Landsat 8, Landsat 9, and Sentinel-2 MSI imagery. To calculate water quality parameters, users can select individual indicators, such as TSS, turbidity, COD, BOD5, NH4+, and Land Surface Temperature (LST).

Findings. Spatial distribution of TSS and turbidity in the Red River and Duong River. TSS concentration. In this study, three Sentinel-2 MSI images captured on December 19, 2023, May 3, 2024, and December 19, 2024, were used to determine TSS concentrations in the surface waters of the Red River and Duong River segments flowing through Hanoi. Selecting image acquisition dates that represent different hydrological conditions enables an assessment of the spatial and temporal variations in TSS within the study area. The processing and calculation of TSS concentrations were implemented entirely on the GEE platform using the tool/application developed in this research. Within this platform, Sentinel-2 MSI images were accessed directly from GEE's global remote sensing data repository and then filtered by study area and acquisition time to ensure consistency across the images. The study uses the Near-Infrared (NIR; Band 8), Blue (Band 2), and Green (Band 3) spectral bands of Sentinel-2A imagery to generate spectral ratio images, specifically NIR/Blue and NIR/Green. These ratio images were computed directly on GEE using the JavaScript programming environment (Code Editor) and subsequently converted into TSS concentrations based on the empirical relationships established in this research.

Implementing the processing workflow on GEE offers numerous advantages over traditional image processing methods. All computations, including spectral band extraction, spectral ratio calculation, application of TSS determination formulas, and generation of output raster layers, are performed automatically on Google's server infrastructure. This helps standardize the processing workflow across different image acquisition dates and significantly reduces processing time and effort compared with local processing using traditional methods.

Fig. 5. User interface of the Google Earth Engine application for estimating surface-water quality parameters from satellite imagery

Table 1

Comparison of total suspended solids (TSS) concentrations derived from Sentinel-2 MSI imagery and measured in water samples

No.	Coordinates		TSS concentration, mg/l		Difference, mg/l
	X, m	*Y*, m	Identification from Sentinel 2A image	Sampling results	
1	584,228	2,332,580	22.48	22.81	–0.33
2	585,768	2,332,214	20.61	21.55	–0.94
3	592,549	2,331,080	19.67	21.7	–2.03
4	584,517	2,332,564	24.59	20.62	3.97
5	584,297	2,332,568	22.88	19.43	3.45
6	583,791	2,332,547	20.25	23.5	–3.25
7	583,327	2,332,646	21.79	18.54	3.17
8	582,870	2,332,712	22.95	17.49	5.46
9	582,662	2,332,752	22.15	18.04	4.11
10	581,776	2,333,145	22.91	26.5	–3.49

In addition to generating raster layers for mapping TSS distribution, GEE enables rapid extraction of TSS values at specific validation points using sampling functions. This facilitates validation by comparing results with field observations and sampling data (Table 1).

Fig. 6 presents TSS concentrations in the surface water of the Red River and Duong River segments flowing through Hanoi. TSS concentrations are grouped into 11 intervals: less than 16 mg/l; 16–18; 18–20; 20–22; 22–24; 24–26; 26–28; 28–30; 30–32; 32–36 mg/l; and greater than 36 mg/l. The analysis indicates that TSS concentrations in the surface water of the Red River and Duong River segments primarily range from 18 to 30 mg/l. Surface water near the banks tends to have higher TSS concentrations than mid-river areas, reflecting the influence of nearshore currents, discharge, and sand mining. High TSS concentrations are also recorded at the confluence of the Red and Duong Rivers. Areas with TSS concentrations exceeding 36 mg/l are localized, mainly near discharge outlets, sand mining sites, and several small tributaries of the Red River upstream of the Thang Long Bridge.

To evaluate the accuracy of TSS concentrations derived from remote sensing imagery, the study used observations from 10 water-quality sampling points in addition to the coefficient of determination (R2). The comparison between TSS concentrations derived from Sentinel-2A imagery and water-sample analysis results is presented in Table 1. At the validation points, the discrepancy between the two data sources ranged from 1.47 to 23.79 %. This indicates that Sentinel-2A imagery, combined with the GEE processing workflow, can determine TSS concentrations in the study area's surface waters with high reliability, meeting the requirements for water-quality monitoring at the river-basin scale.

Turbidity concentration. Similar to the TSS parameter, the turbidity distribution map for the surface waters of the Red River and Duong River was developed using the image-processing tool on the GEE platform established in this study. In GEE, Sentinel-2A imagery was filtered based on the study area and acquisition time, and the required spectral bands were extracted. The spectral ratios (NIR/Blue) and (NIR/Green) were then calculated as inputs for turbidity determination. The entire processing chain was implemented within the GEE Code Editor/application environment, enabling automation from data access and ratio image calculation to conversion to turbidity values and visualization as map layers. The resulting turbidity distribution map is shown in Fig. 7, and Nephelometric Turbidity Unit (NTU) val-

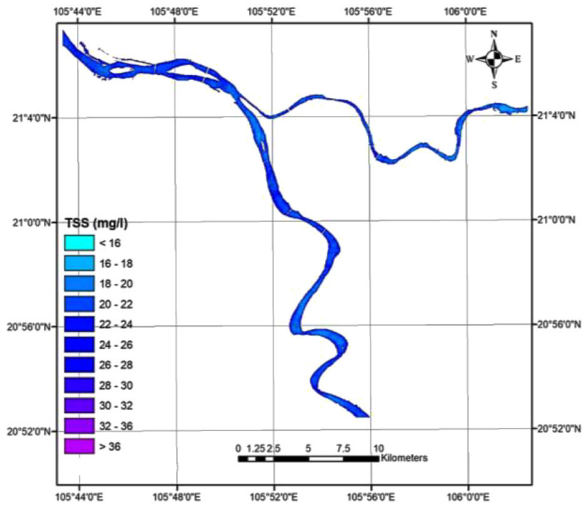

Fig. 6. Spatial distribution of TSS concentration derived from Sentinel-2 MSI imagery acquired on December 19, 2023

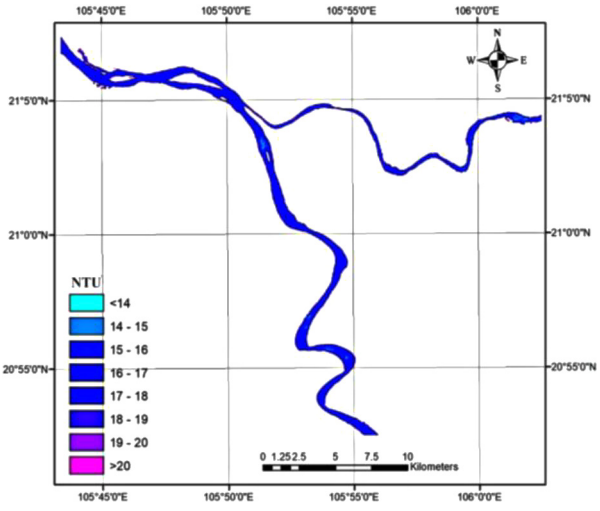

Fig. 7. Spatial distribution of turbidity derived from Sentinel-2 MSI imagery acquired on December 19, 2023

Table 2

Comparison of turbidity values derived from Sentinel-2 MSI imagery and measured in water samples

No.	Coordinates		NTU Concentration, mg/l		Difference, mg/l
	X, m	Y, m	Identification from Sentinel 2A image	Sampling results	
1	584,228	2,332,580	15.76	19.01	–3.25
2	585,768	2,332,214	15.41	17.66	–2.25
3	592,549	2,331,080	15.20	13.7	1.50
4	584,517	2,332,564	15.98	13.93	2.05
5	584,297	2,332,568	16.57	11.96	4.61
6	583,791	2,332,547	15.56	15.36	0.20
7	583,327	2,332,646	16.17	15.58	0.59
8	582,870	2,332,712	15.57	11.355	4.22
9	582,662	2,332,752	16.37	13.705	2.66
10	581,776	2,333,145	16.49	18.55	–2.06

ues at validation points can be rapidly extracted for comparison with observational data, as presented in Table 2.

In Fig. 7, turbidity concentrations are grouped into eight intervals: less than 14 NTU, 14-15 NTU, 15-16 NTU, 16-17 NTU, 17-18 NTU, 18-19 NTU, 19-20 NTU, and greater than 20 NTU. The analysis indicates that for most segments of the Red and Duong Rivers flowing through Hanoi, turbidity ranges from 14 to 18 NTU. Areas with turbidity below 14 NTU are small and locally distributed in the middle of the river. In contrast, areas with turbidity exceeding 18 NTU are primarily located along the riverbanks, consistent with flow dynamics and the influence of riparian discharge. The accuracy of the turbidity concentrations derived from Sentinel-2A imagery was also evaluated using 10 validation points. The comparison between satellite-derived turbidity and water sample analysis data (Table 2) shows discrepancies ranging from 0.20 to 4.61 NTU, corresponding to a maximum deviation of approximately 28%. These results demonstrate that the GEE-based image-processing workflow effectively captures the spatial distribution of surface water turbidity in the study area, meeting the requirements for water quality monitoring and assessment at the river-basin scale.

Results of water surface temperature determination from Landsat 8/9 remote sensing data. Data and processing procedures on GEE. Water Surface Temperature (WST) is a critical parameter that reflects the thermal state of a water body. It is closely linked to hydrodynamic and biochemical processes and to the overall quality of the aquatic environment. In this study, the water surface temperature distribution for the Red River and Duong River areas was determined and analyzed on the GEE platform using Landsat 8 and Landsat 9 remote sensing imagery. Two Landsat scenes were used: a Landsat 8 OLI/TIRS image captured on September 6, 2024 (representing the rainy season) and a Landsat 9 OLI/TIRS image captured on December 19, 2024 (representing the dry season). On the GEE platform, Landsat imagery was accessed directly from the global remote sensing data repository, then filtered by study area and acquisition time. The image processing chain was developed and executed automatically within the Code Editor (JavaScript) environment, encompassing the following key steps:

- pre-processing and selection of thermal bands;
- conversion of digital numbers (DN) to spectral radiance;
- calculation of brightness temperature and emissivity correction to determine water surface temperature;
- clipping the results to the boundaries of the Red River and Duong River basins;
- classification and visualization of results as raster maps.

Implementing the entire workflow on GEE standardizes calculation methods across image acquisition dates. Furthermore, it significantly reduces processing time and effort compared to traditional local processing methods because computations are performed directly on Google's server infrastructure.

Results of water surface temperature distribution. The water surface temperature results for the study area, derived from Landsat 8 imagery (September 6, 2024) and Landsat 9 imagery (December 19, 2024), are presented in Figs. 8 and 9. For spatial analysis, the water surface temperature is categorized into five value intervals: less than 20, 20–22, 22–24, 24–26 °C, and greater than 26 °C.

The analysis indicates that water surface temperatures in the Red and Duong River segments flowing through Hanoi are generally below 28 °C and show a distinct difference between the rainy and dry seasons. Specifically, on September 6, 2024 (rainy season), most of the water surface in the study area had temperatures below 22 °C, shown as dark blue on the map (Fig. 8). Areas with temperatures exceeding 24 °C were limited

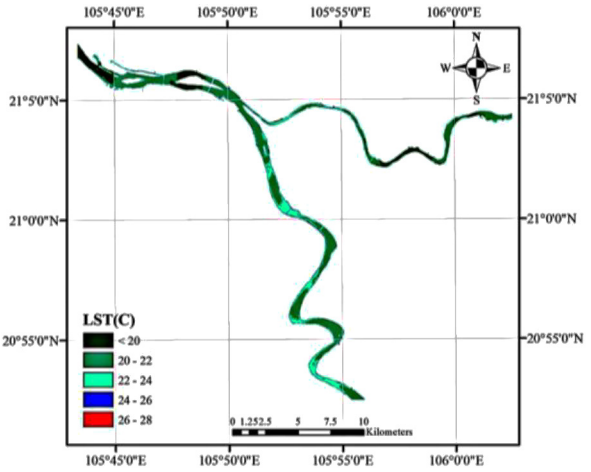

Fig. 8. Spatial distribution of water surface temperature derived from Landsat 8 OLI/TIRS imagery acquired on September 6, 2024

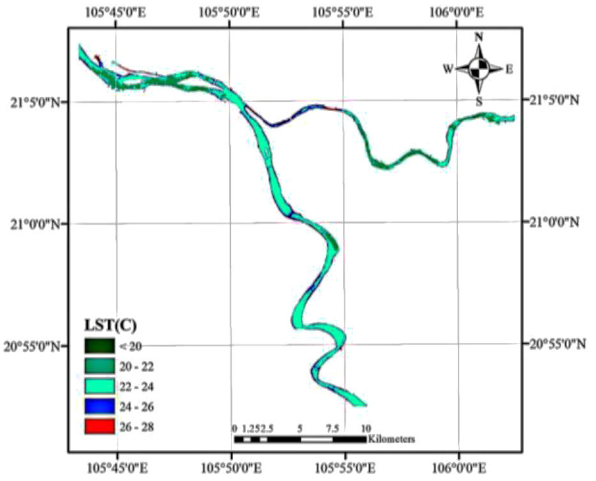

Fig. 9. Spatial distribution of water surface temperature derived from Landsat 9 OLI/TIRS imagery acquired on December 19, 2024

and scattered along certain banks of the Red and Duong Rivers. Conversely, on December 19, 2024 (dry season), water surface temperatures were generally higher, with most of the study area ranging from 22–24 °C, shown as blue on the map (Fig. 9). Some areas with surface temperatures above 24 °C were primarily located in the Duong River basin, several small tributaries of the Red River, and nearshore waters.

Discussion. The research results demonstrate that the GEE platform plays a central role in automating and standardizing the entire surface water quality monitoring workflow for the Red River and Duong River basins. Directly leveraging multi-source remote sensing data repositories (Sentinel-2 MSI, Landsat 8/9) on GEE enables rapid access to imagery within the study's spatial and temporal scope, eliminating the need for the complex data downloading, storage, and preprocessing steps required by traditional methods. In this study, GEE was used not only as a remote sensing image-processing tool but also as an integrated platform that combines remote sensing data, field observation data, and a programming environment (JavaScript) to develop a water quality monitoring application. The processing chain, ranging from spatial filtering and spectral band extraction to calculating spectral ratios, converting them into water quality parameters (TSS, turbidity), and determining water surface temperature, was executed automatically and consistently on GEE. This minimizes discrepancies arising from manual operations while ensuring the methodology's reproducibility and scalability.

The distribution maps of TSS and turbidity show significant spatial variation across the Red and Duong Rivers, reflecting the combined effects of hydrological conditions, river morphology, and socioeconomic activities along the riverbanks. The higher TSS and turbidity levels observed in nearshore areas, near discharge outlets, at sand-mining sites, and at the confluence of the Red and Duong Rivers are consistent with the study area's characteristics. Comparisons with observational data at 10 validation points indicate that discrepancies between Sentinel-2-derived values and water-sample analysis results fall within an acceptable range. For TSS, the discrepancy ranged from 1.47 to 23.79 %, while for turbidity, the maximum deviation was approximately 28 %. These discrepancies may stem from time differences between satellite overpass and field sampling, atmospheric effects, and the heterogeneity of the surface water environment at the time of observation. However, for water quality monitoring at the river basin scale, the results demonstrate that the methodology using Sentinel-2 imagery in combination with the GEE processing workflow is relatively reliable and effectively captures the spatial distribution trends of water quality parameters.

Determining water surface temperature from Landsat 8/9 data on the GEE platform reveals a clear distinction between the rainy and dry seasons in the study area. Lower water surface temperatures during the rainy season and higher temperatures during the dry season align with the hydro-climatological patterns of the Red River basin. The spatial distribution of water surface temperature also highlights the influence of flow characteristics, river morphology, and nearshore areas. Using GEE for Landsat data processing standardizes water surface temperature calculation methods across periods and facilitates long-term time-series analysis. This is particularly significant for monitoring surface water temperature fluctuations related to climate change and the impacts of socio-economic development activities within the river basin.

Compared to traditional remote sensing image processing methods based on local software, the application of GEE in this study offers several distinct advantages. First, GEE significantly reduces processing time and costs because all computations are performed on cloud computing infrastructure. Additionally, the built-in integration of multi-temporal and multi-source remote sensing datasets enables flexible and consistent analysis. Developing a monitoring application on GEE enables users to easily select data, timeframes, and parameters for analysis, thereby enhancing its practical applicability in water management. However, the remote sensing and GEE-based approach still has certain limitations, such as dependence on weather conditions (cloud cover), the spatial resolution of satellite imagery, and the need for calibration and validation using field observation data. Therefore, combining remote sensing data with traditional monitoring data remains an essential approach to improving the accuracy and reliability of monitoring results.

Conclusion. This study developed and implemented a cloud-based application for surface water quality monitoring on the GEE platform, integrating multi-source satellite data and in situ measurements. The approach was tested in the Red River and Duong River sections flowing through Hanoi to provide an efficient, automated solution for spatiotemporal water quality assessment at the river-basin scale. Sentinel-2 MSI imagery was used to estimate total suspended solids and turbidity, while Landsat 8/9 thermal data were used to derive water surface temperature. All processing steps, including data access, spectral band extraction, index calculation, parameter retrieval, and visualization, were performed automatically in the GEE cloud environment. The results show that the spatial distributions of TSS, turbidity, and water surface temperature align with hydrological conditions and field measurements, with acceptable differences between satellite-derived estimates and in situ data. The study demonstrates that GEE is an effective platform for building scalable, user-

friendly water quality monitoring applications, offering significant advantages in processing efficiency and data accessibility compared with traditional desktop-based methods. Future work will focus on extending the application to other river basins, incorporating additional water quality parameters, and integrating advanced machine learning techniques and near-real-time monitoring capabilities to further improve accuracy and operational applicability.

References.

1. Djumaboev, K., Anarbekov, O., Holmatov, B., Hamidov, A., Gafurov, Z., Murzaeva, M., & Smakhtin, V. (2019). Surface water resources. *The Aral Sea Basin*, 25-38. https://doi.org/10.4324/9780429436475

2. Amralinova, B., Agaliyeva, B., Lozynskyi, V., Frolova, O., Rysbekov, K., Mataibaeva, I., & Mizernaya, M. (2023). Rare-Metal Mineralization in Salt Lakes and the Linkage with Composition of Granites: Evidence from Burabay Rock Mass. *Water, 15*(7), 1386. https://doi.org/10.3390/w15071386

3. Ramli, M., Sufriadin, Saputra, A., & Nurhikmah (2025). Hydrochemical analysis of surface water flow from an abandoned iron ore mine. *Mining of Mineral Deposits, 19*(1), 65-71. https://doi.org/10.33271/mining19.01.065

4. Absametov, M., Ismagulova, A., Mirlas, V., Kulagin, V., Umbetaliev, D., Rakhimov, T., & Rakhimova, V. (2025). Monitoring of the water and salt balance of the Bakbakty rice irrigation system under reuse of collector-drainage water for irrigation. *Engineering Journal of Satbayev University, 147*(3), 40-47. https://doi.org/10.51301/ejsu.2025.i3.06

5. Popovych, V., Skrobala, V., Tyndyk, O., & Kaspruk, O. (2024). Hydro-ecological monitoring of heavy metal pollution of water bodies in the Western Bug River basin within the mining-industrial region. *Mining of Mineral Deposits, 18*(4), 139-152. https://doi.org/10.33271/mining18.04.139

6. Nasiedkin, Ye. I., Olshtynska, O. P., Stadnichenko, S. M., Ivanova, G. M., Yemelianov, V. O., Dovbysh, S. M., & Fedoseienkov, S. G. (2024). Monitoring of suspended matter in the Dnipro River within Zaporizhzhia city, main trends of 2022. *Mineral Resources of Ukraine*, (3), 69-72. https://doi.org/10.31996/mru.2024.3.69-72

7. Loucks, D. P., & van Beek, E. (2017). Water Resources Planning and Management: An Overview. *Water Resource Systems Planning and Management*, 1-49. https://doi.org/10.1007/978-3-319-44234-1_1

8. van Vliet, M. T. H., Thorslund, J., Strokal, M., Hofstra, N., Flörke, M., Ehalt Macedo, H., Nkwasa, A., ..., & Mosley, L. M. (2023). Global river water quality under climate change and hydroclimatic extremes. *Nature Reviews Earth & Environment, 4*(10), 687-702. https://doi.org/10.1038/s43017-023-00472-3

9. Ahmed, U., Mumtaz, R., Anwar, H., Mumtaz, S., & Qamar, A. M. (2019). Water quality monitoring: from conventional to emerging technologies. *Water Supply, 20*(1), 28-45. https://doi.org/10.2166/ws.2019.144

10. Aluwong, K. C., Hashim, M. H. M., Ismail, S., & Shehu, S. A. (2024). Physico-chemical assessment of surface water from mining activities in Maiganga coal mine, Gombe state, Nigeria. *Mining of Mineral Deposits, 18*(1), 9-17. https://doi.org/10.33271/mining18.01.009

11. Zaidi Farouk, M. I. H., Jamil, Z., & Abdul Latip, M. F. (2023). Towards online surface water quality monitoring technology: A review. *Environmental Research, 238*, 117147. https://doi.org/10.1016/j.envres.2023.117147

12. Khalil, B., & Ouarda, T. B. M. J. (2009). Statistical approaches used to assess and redesign surface water-quality-monitoring networks. *Journal of Environmental Monitoring, 11*(11), 1915. https://doi.org/10.1039/b909521g

13. Khalil, B., Ouarda, T. B. M. J., St-Hilaire, A., & Chebana, F. (2010). A statistical approach for the rationalization of water quality indicators in surface water quality monitoring networks. *Journal of Hydrology, 386*(1-4), 173-185. https://doi.org/10.1016/j.jhydrol.2010.03.019

14. Nguyen, M. H., Tran, T. A., Tap Van, H., Hoang, T. H. N., Phan, P. C. M., Nguyen, C. L., Nguyen, D. T., & Pham, T. H. (2023). Surface water quality assessment in the Bach Dang river basin, Vietnam: using water quality index and geographical information system methods. *Environmental Research Communications, 5*(7), 75015. https://doi.org/10.1088/2515-7620/ace87e

15. Saab, C., & Zéhil, G.P. (2025). Statistical analysis techniques in water quality monitoring: a review. *Stochastic Environmental Research and Risk Assessment, 39*(9), 3723-3760. https://doi.org/10.1007/s00477-025-03035-8

16. Sagan, V., Peterson, K. T., Maimaitijiang, M., Sidike, P., Sloan, J., Greeling, B. A., Maalouf, S., & Adams, C. (2020). Monitoring inland water quality using remote sensing: potential and limitations of spectral indices, bio-optical simulations, machine learning, and cloud computing. *Earth-Science Reviews, 205*, 103187. https://doi.org/10.1016/j.earscirev.2020.103187

17. Ramadas, M., & Samantaray, A. K. (2017). Applications of Remote Sensing and GIS in Water Quality Monitoring and Remediation: A State-of-the-Art Review. *Water Remediation*, 225-246. https://doi.org/10.1007/978-981-10-7551-3_13

18. Amani, M., Ghorbanian, A., Ahmadi, S. A., Kakooei, M., Moghimi, A., Mirmazloumi, S. M., Moghaddam, ..., & Brisco, B. (2020). Google Earth Engine Cloud Computing Platform for Remote Sensing Big Data Applications: A Comprehensive Review. *IEEE Journal of Selected Topics in Applied Earth Observations and Remote Sensing, 13*, 5326-5350. https://doi.org/10.1109/jstars.2020.3021052

19. Zhao, Q., Yu, L., Li, X., Peng, D., Zhang, Y., & Gong, P. (2021). Progress and Trends in the Application of Google Earth and Google Earth Engine. *Remote Sensing, 13*(18), 3778. https://doi.org/10.3390/rs13183778

20. Jahangeer, J., Joshi, P., Kapoor, A., & Tang, Z. (2025). A review of AI-driven Google Earth Engine applications in surface water monitoring, assessment, and management. *Discover Geoscience, 3*(1). https://doi.org/10.1007/s44288-025-00255-x

21. Hasan, R., Kapoor, A., Singh, R., & Yadav, B. K. (2024). A state-of-the-art review on the quantitative and qualitative assessment of water resources using google earth engine. *Environmental Monitoring and Assessment, 196*(12). https://doi.org/10.1007/s10661-024-13315-5

22. Das, S., Nandi, D., Thakur, R.R., Bera, D.K., Behera, D., Đurin, B., & Cetl, V. (2024). A Novel Approach for Ex Situ Water Quality Monitoring Using the Google Earth Engine and Spectral Indices in Chilika Lake, Odisha, India. *ISPRS International Journal of Geo-Information, 13*(11), 381. https://doi.org/10.3390/ijgi13110381

23. Dey, S., & Dutta Roy, A. (2025). Satellite-Based Monitoring of Water Quality in Mukutmanipur Dam: A Google Earth Engine Approach. *Remotely Sensed Rivers in the Age of Anthropocene*, 637-657. https://doi.org/10.1007/978-3-031-82311-4_25

24. Navabian, M., Vazifedoust, M., & Varaki, M.E. (2023). *A multi-sensor framework in google earth engine for spatio-temporal trend analysis of water quality parameters in Anzali lagoon*. Preprint. https://doi.org/10.21203/rs.3.rs-3335434/v1

25. Atiz, O. F., & Durduran, S. (2025). Assessing long-term hydrological dynamics and water quality using Google Earth Engine: A case study of Ilgın Lake (1985–2024). *The International Archives of the Photogrammetry, Remote Sensing and Spatial Information Sciences, XL-VIII-4/W13-2025*, 33-39. https://doi.org/10.5194/isprs-archives-xlviii-4-w13-2025-33-2025

26. Tran, M. C., Nguyen, T. G., Tran, A. P., & Nguyen, A. D. (2025). Application of the Otsu algorithm on the Google Earth Engine platform for monitoring reservoir operation in the transboundary Da River basin using satellite and topographic data. *Vietnam Journal of Hydrometeorology*, (770), 84-96. https://doi.org/10.36335/VNJHM.2025(770).84-96

27. Vu, H. L., Nguyen, V. G., Trinh, P. H., & Pham, V. H. (2019). Applying Google Earth Engine in river bank erosion monitoring: A case study in the Lower Mekong River. *Ho Chi Minh City University of Education Journal of Science, 16*(6), 38-49. https://doi.org/10.54607/hcmue.js.16.6.2507(2019)

28. Tran, T. T., & Tran, D. H. (2023). Applying Google Earth Engine and DSAS for automated shoreline monitoring: A case study of Cua Tung, Quang Tri Province. *Journal of Hydraulic Science and Technology*, (80), 59-68. https://vjol.info.vn/vawr/en/article/view/99942/84307/

29. Phạm, V. A., Le, T. H., Nguyen, T. H., Bui, Q. T., Vũ, P. L., & Phạm, V. M. (2024). Monitoring river morphological dynamics using multitemporal image and GIS technology. *Proceedings of the 2020 National GIS Application Conference*, 1-12 https://www.researchgate.net/publication/358504663

30. Nguyen, T. T. H., Bui, D. C., Nguyen, T. P. T., & Bui, T. N. (2016). First experience in modeling spatial distribution of chlorophyll-a concentration and TSI in the West Lake water using Sentinel-2A image. *VNU Journal of Science: Earth and Environmental Sciences, 32*(2S), 121-130.

Застосування Google Earth Engine для автоматизованого моніторингу якості поверхневих вод у басейнах річок Хонгха та Дуонг

Л. Т. Дінг[1], *Т. Т. Х. Дінг*[*2], *К. Т. Тран*[3], *В. Б. До*[3]

1 – Інститут механіки, автоматизації, екологічних наук і технологій, м. Ханой, В'єтнам
2 – Університет електроенергетики, м. Ханой, В'єтнам
3 – Ханойський університет гірничої справи та геології, м. Ханой, В'єтнам
[*] Автор-кореспондент e-mail: hiendtt@epu.edu.vn

Мета. Розробити автоматизований хмарний застосунок для моніторингу якості поверхневих вод із використанням Google Earth Engine та мультисенсорних супутникових даних, орієнтований на великі річкові системи й апробований на прикладі річок Хонгха та Дуонг у В'єтнамі.

Методика. Дослідження проведене із використанням мультисенсорних супутникових даних Sentinel-2 MSI і Landsat 8/9 у середовищі Google Earth Engine. За даними Sentinel-2 MSI визначали вміст завислих речовин (TSS) і каламутність води, тоді як теплові канали Landsat 8/9 використовували для розрахунку температури водної поверхні. Оброблення даних передбачало фільтрацію супутникових зображень за територією та часом знімання, спектральний аналіз, розрахунок відповідних показників якості води й картографічну візуалізацію їх просторового розподілу. Отримані за супутниковими даними значення порівнювали із результатами натурних вимірювань на ділянках річок Хонгха й Дуонг у межах Ханоя, В'єтнам.

Результати. Встановлені виразні просторові й сезонні закономірності зміни вмісту завислих речовин, каламутності й температури водної поверхні. Порівняння результатів, отриманих за супутниковими даними, із результатами натурних вимірювань показало прийнятну узгодженість, що підтверджує придатність запропонованого підходу для оцінювання якості води в масштабах річкових басейнів.

Наукова новизна. Запропоновано інтегрований підхід на основі Google Earth Engine, що поєднує мультисенсорні дані дистанційного зондування Землі із результатами натурних спостережень і забезпечує автоматизований і масштабований моніторинг якості поверхневих вод у В'єтнамі.

Практична значимість. Розроблений застосунок може бути ефективно використаний для оперативного, масштабованого й економічно доцільного моніторингу якості води, особливо в регіонах із дефіцитом даних і великих річкових басейнах, де можливості традиційних мереж спостережень є обмеженими.

Ключові слова: *Google Earth Engine, зондування Землі, якість води, завислі речовини, каламутність, річковий басейн*